

UDK 622.785:621.927:519.718:541.45

Synthesis and Sintering of Ceramic Nanocomposites with High Mixed Conductivity

V. V. Zyryanov*, V.A. Sadykov¹, M.I. Ivanovskaya², J.M. Criado³, S. Neophytides⁴

Institute of Solid State Chemistry SB RAS, Novosibirsk, Russia,

¹Boreskov Institute of Catalysis SB RAS, Novosibirsk, Russia,

²Institute of Physicochemical Problems, BSU, Minsk, Byelorussia,

³Institute of Materials Science, Seville University, Seville, Spain,

⁴Institute of Chemical Engineering & High Temperature Processes, Patras, Greece

Abstract:

Metastable solid solutions of complex oxides with fluorite and perovskite structures are obtained by mechanosynthesis. Dense ceramics on the base of these metastable phases was obtained by thermal sintering of nanopowders due to kinetic stabilization. Different degrees of a chemical interaction (interdiffusion) are observed during sintering of "perovskite+fluorite" and "perovskite+perovskite" composites. It is shown, that optimization of the composition, mixing conditions of individual phases and their sintering, preparation of ceramic composites with mixed conductivity for use in catalytic membrane reactors is possible. Unusual behavior of complex perovskites and fluorites is discovered during sintering, enabling determination of an optimum sintering temperature and time for which a qualitative explanation is given. It is established that rearrangement of fine crystalline particles as a whole plays a key role in shrinkage.

Keywords: *Mechanosynthesis, complex oxides, perovskites, fluorites, composites, ceramics, sintering, interdiffusion, mixed conductivity.*

1. Introduction

Dense ceramic membranes with high mixed oxygen-ion and electron conduction and the catalytic membrane reactors based on them are under thorough investigation because of promising applications of highly efficient and ecologically pure large-scale technologies connected mainly with natural gas processing. In order to provide high oxygen permeability, which is the main parameter of the membrane, it is necessary that the ionic and electron conductivities were comparable in transport numbers, and the surface reaction of oxygen exchange should be rather fast not to limit the process. The electron conduction is usually much higher than the ionic one, so, as a rule, ionic conductivity of the membrane material determines its permeability. The most studied mixed conductors are based on SrFeO₃ and LaCoO₃ solid solutions with a perovskite structure [1-2]. For example, La_{1-x}(Sr,Ca)_xCo_{1-y}Fe_yO_{3-z} possesses very high electron conductivity and rather high ionic conductivity, which is an order of magnitude higher than that in yttria stabilized zirconia [3]. The highest permeability is likely to be obtained by Ishihara in perovskite

*) Corresponding author: vladi@mail.nsk.ru

$\text{La}_{0.7}\text{Sr}_{0.3}\text{Ga}_{0.6}\text{Fe}_{0.4}\text{O}_{3-x}$, where the flow $8,2 \mu\text{mol cm}^{-2}\text{s}^{-1}$ was achieved in a membrane 0,3 mm thick at 1000 °C [4]. It should be noted that one of the best ionic conductors is perovskite $\text{La}_{0.8}\text{Sr}_{0.2}\text{Ga}_{0.8}\text{Mg}_{0.2}\text{O}_{3-x}$, whose doping with cations of variable valence leads to the appearance of substantial electron conductivity, and finally high permeability.

High mixed conductivity was also discovered in layered perovskites like La_2NiO_4 [5], in Ruddlesden-Popper phases $\text{Sr}_3\text{M}_2\text{O}_{7-x}$ (M=Ti,Co,Fe,Mn) [6] and in the so-called Balachandran phase $\text{Sr}_2\text{Fe}_2\text{CoO}_x$ [7]. Mixed-type conductors with a fluorite structure are mainly represented by solid solutions based on CeO_2 and Bi_2O_3 with Pr or Tb additives [8]. However, the use of membranes with mixed conductivity is restricted by a number of disadvantages of membrane materials known at present. The most essential among them are poor mechanical characteristics, instability under reaction conditions, and low stability to thermal shocks. In addition, the majority of the listed compounds undergo reduction in a medium containing methane and hydrogen, followed by degradation or carbonization of the surface. As a rule, membranes with high conductance are characterized by a low rate of the oxygen exchange reaction at the surface. High temperature of sintering is characteristic for membranes based on CeO_2 . Rare earths and LaGaO_3 -based membranes are too expensive. Finally, membranes made of conductors with mixed conductivity exhibit insufficient oxygen permeability and stability to provide an actual replacement for the industrial process of steam conversion of methane.

Another group of materials is represented by the so-called two-phase composites involving ionic and electronic conductors. For this type of mixed-type conductors, there is a possibility to choose the best ion and electron conductors as the components of the composite and to adjust mixed conduction by changing their ratio.

The best-studied composites are based on the solid electrolyte $\text{Ce}_{0.8}\text{Gd}_{0.2}\text{O}_{2-x}$ with a fluorite structure. Perovskites $\text{La}_{0.7}\text{Sr}_{0.3}\text{MnO}_3$ [9] and $\text{Gd}_{0.7}\text{Ca}_{0.3}\text{CoO}_3$ [10], spinel MFe_2O_4 (M=Co, Mn) [4] were used in composites as the electronic conductors. Oxygen flow of $7 \mu\text{mol cm}^{-2}\text{s}^{-1}$ at 1000 °C was obtained in [4] with the volume fraction of the electron-type conductor of 15% in 0.24 mm membrane. Promising results within an intermediate temperature range were obtained in the composite from ionic $\text{Bi}_{0.75}\text{Y}_{0.25}\text{O}_{1.5}$ and electronic $\text{Bi}_2\text{CuO}_{4-x}$ conductors [11]. High mixed conductivity in the same temperature range was also observed in composites with a BaBiO_3 rhombohedral phase in Ba-Sr-Bi-O or Ba-Sr-Ca-Bi-O systems [12-13].

However, additional problems arise in the development of composites with mixed conductivity. The most important problem is interdiffusion or chemical interaction between the components during sintering. In order to obtain dense membranes on a porous substrate, it is necessary to use nano-size powders with high sintering activity, since only in this case the sintering temperature can be reduced below 1300 °C for Bi_2O_3 -free conductors. Above this temperature, porous substrates derived from corundum, cermet or heat-resisting alloys undergo densification during sintering. On the other hand, it is very difficult to ensure high permeability in thick self-supported membranes. Nano-sized powders of various phases also exhibit high reactivity along with sintering activity. Previously we investigated [14-16] a series of composites like perovskite + fluorite (P+F) and perovskite + perovskite (P+P) derived by mechanochemical synthesis. It was demonstrated that a chemical interaction proceeds during sintering in all composites but to a quite different degree. It should be noted that powders of mechanochemical origin have some specific features [16-17]. Powder morphology possesses a strong hierarchy, which has been established by a combination of adsorption methods and EM [16-18]. The structure is characterized by anti-glass type disordering, that is, long-range order (X-ray diffraction patterns with high space symmetry, as a rule, F m3m for fluorites and P 3m3 for perovskites, and crystallite sizes estimated from broadened peaks are about 5 – 50 nm) is accompanied by weak short-range ordering, exhibiting a low point symmetry with the appearance of bands in the IR and Raman spectra which are prohibited for these space groups [19]. The powders are composed of aggregates with a size up to $\sim 1 \mu\text{m}$

and density ~80%, which are nanocomposites of crystallites in an amorphous matrix. In turn, these nano-sized crystallites are composed of domains, twins and have a density reduced to ~90% due to strong disordering and high content of vacancies. The aggregates form secondary agglomerates with a size up to 100 μm and density 65-75%. Such morphology of mechanochemical powders renders special advantages to them: it provides high sintering activity and unique possibilities for compacting till the density of ~70% by means of usual pressing or casting [18], and also the possibility to obtain porous ceramics with high strength [20]. At the same time, binary mixed oxides derived by mechanosynthesis are usually metastable and undergo structural transformations during annealing. This disadvantage of mechanochemical powders was eliminated in [15-16] by complex doping due to kinetic stabilization of metastable phases. One may expect that complex doping will improve the compatibility of components in the composite with respect to many parameters, affect the rate of the surface exchange reaction, etc.

Experimental

Mixed oxides with a perovskite and fluorite structure as components of composites were derived by mechanosynthesis in an AGO-2 planetary mill using a correct procedure of mechanical treatment [18]. This procedure provides contamination reduction from 2-3 orders down to $<5 \cdot 10^{-2} \%$ and macro-uniformity of the powders. The charge of oxide mixture and 9 mm steel balls was 15/220 g. After 20 min treatment in a planetary mill, the powders were subjected to disagglomeration and separation in a micro-separator of the EMC type, POLYPROM, Ekaterinburg. The fine fraction with the aggregate size $< 1 - 2 \mu\text{m}$ was used to obtain ceramics. The composites were prepared by homogenization of nanopowders derived by mechanosynthesis in a planetary micro-mill from hard alloy WC/Co containing one milling body. The powders were compacted into discs 12 mm in diameter and 2 mm thick by uniaxial pressing at 100 MPa. Sintering of the samples was carried out in air at 1100-1250 $^{\circ}\text{C}$ with cooling in the furnace. The density of the samples was measured using Archimedes' method.

DRON-3M installation with Cu K_{α} radiation was used to record the powder diffraction patterns. The data were collected in a range $2\theta = 8 - 84^{\circ}$ with a step of 0.01° . In order to reduce the effect of non-uniformity of the samples, the diffraction patterns were recorded 2 and more times with repeated filling of the cell. Powder Cell 2.4 software was used for structure calculations. The positions of broadened reflections were determined in the approximation of Lorenz's form of lines, which provides the best description for peaks in non-uniform powders, derived by mechanosynthesis.

Results and Discussion

Structure parameters of complex perovskites and fluorites derived by mechanosynthesis are presented in table I. Diffraction patterns of some solid solutions before and after sintering are shown in Fig. 1. Kinetic stabilization of the disordered metastable phases is really achieved by complex doping which inhibits the nucleation stage of the stable phases. Complex solid solutions keep their structure after sintering up to dense ceramics without open pores. Moreover, by selecting the compositions we reduced the difference in sintering temperatures of components and simultaneously decreased chemical interactions during sintering in some composites. The parameters of the investigated composites are

shown in Table 2. Diffraction patterns in Fig. 2 and 3 display interactions between components during sintering of composites through changes in cell parameters.

Table I Parameters of perovskites (P) and fluorites (F), derived by mechanosynthesis and after sintering.

Sample (T _c , °C)	Composition	Cell parameter, Å	Width of (111) peak, 2θ	Grain size, nm
F1	Bi _{0.40} Ca _{0.1} Y _{0.1} In _{0.1} La _{0.1} Pr _{0.1} Ce _{0.1} O _{1.5}	5.462(6)	0.592	40
F1T(1100)	-II-	5.500(1)	0.183	420
F2	Bi _{0.35} La _{0.35} Pr _{0.15} Sr _{0.05} Ca _{0.05} Sm _{0.05} O _{1.45}	5.601(4)	0.49	52
F2T(1100)	-II-	a=3.904(1); c=9.870(2)	0.172	590
F3	Bi _{0.35} La _{0.3} Sr _{0.1} Pr _{0.1} Sm _{0.1} Gd _{0.05} Y _{0.05} O _{1.45}	5.567(3)	0.535	46
F3T(1100)	-II-	a=3.890(1); c=9.818(2)	0.201	300
F4T(1200)	Ce _{0.7} Pr _{0.3} O _{1.85} *	5.408(3)	0.202	295
F5	Ce _{0.8} Gd _{0.2} O _{1.9}	5.412(2)	0.545	45
F5T(1200)	-II-	5.425(1)	0.17	600
P1	La _{0.8} Sr _{0.2} Ga _{0.8} Mg _{0.2} O _{2.8}	3.909(2)	0.574	43
P1T(1250)	-II-	3.904(1)	0.244	180
P2	La _{0.87} MnO ₃	3.919(4)	1.094	20
P2T(1250)	-II-	a=5.523(1); c=13.324(3)	0.157	>10 ³
P3	Ba _{0.34} La _{0.33} Bi _{0.33} Mn _{0.67} Fe _{0.33} O _{3-δ}	3.918(1)	0.505	52
P3T(1250)	-II-	3.918(1)	0.292	124
P4	Sr _{0.7} La _{0.2} Ba _{0.1} Fe _{0.5} Co _{0.5} O _{3-δ}	3.849(2)	0.82	28
P4T(1250)	-II-	3.859(1)	0.16	940
P5	Ba _{0.34} La _{0.33} Bi _{0.33} MnO _{3-δ}	3.916(1)	0.441	62
P5T(1200)	-II-	3.9216(9)	0.161	900
P6	Sr _{0.34} La _{0.33} Bi _{0.33} MnO _{3-δ}	3.915(1)	0.694	34
P6T(1200)	-II-	3.888(2)	0.289	118
P7	Ca _{0.34} La _{0.33} Bi _{0.33} MnO _{3-δ}	3.893(3)	0.80	29
P7T(1200)	-II-	3.8753(10)	0.169	480
P8	La ₆ Sr ₂ CaBiGa ₆ MgZnFe ₂ O _{27.5}	3,907(2)	0.61	57
P8T(1200)	-II-	3.9042(7)	0.14	>10 ³
P9	La ₄ Ca ₄ Bi ₂ Mn ₆ Fe ₄ O ₂₈	3.891(3)	0.89	31
P9T(1200)	-II-	3,8706(7)	0.16	>10 ³
P10	La ₆ Sr ₂ CaBiGa ₆ MgZnFeCo _{27.5}	3,899(3)	0.64	51
P10T(1200)	-II-	3.8873(13)	0.16	10 ³
P11	La ₄ Sr ₂ Ca ₂ BiYFe ₄ Co ₃ Mn ₂ NiO ₂₈	3,896(3)	1.10	19
P11T(1200)	-II-	3.8585(15)	0.21	300

*- This sample was prepared by the Pechini route. In F2T, F3T и P2T samples the lattice has a rhombohedral distortion.

The degree of interaction between components in the composite directly depends on the contact surface, that is, on the mixing degree. The most efficient mixing of the components may be obtained under mechanical treatment in a planetary micro-mill in which the particle size of about ~ 300 nm (~ mean aggregate size) is achieved during milling. This really occurs, as one can see by comparing the size of crystallites estimated from broadening

of the X-ray reflections using Sherrer's equation, after annealing individual phases and in composites, see Table I and II. Mechanochemical interactions (mixing at the atomic level) are observed in the case of using high energy planetary mills till the formation of an amorphous or one-phase product with the crystallite size $\sim 5 - 50$ nm. Another method of composite preparation without diminution and mechanosynthesis is wet mixing of the components as fine fractions of aggregates $< 1 \mu\text{m}$, separated in the EMC. This method with an adjusted contact surface is the most promising one, including the formation of a "core-shell" type structure at the compacting stage. However, its realization in laboratory investigations is complicated due to the small content of fine fractions $< 1 \mu\text{m}$.

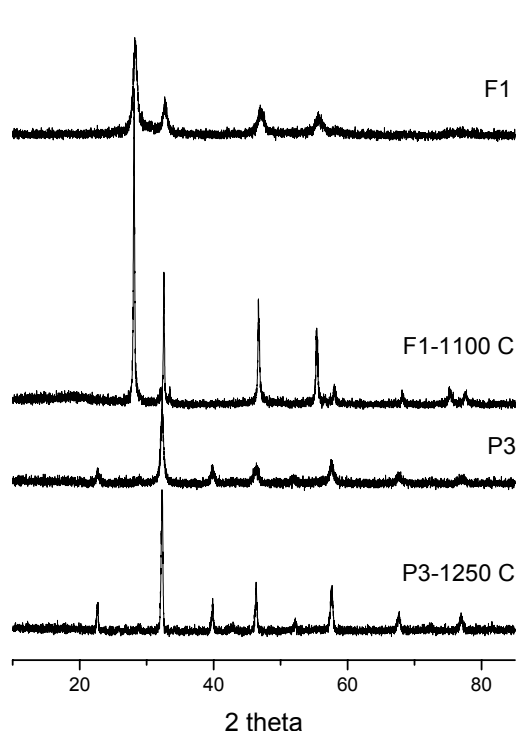


Fig. 1 Diffraction patterns of complex solid solutions with perovskite and fluorite structures derived by mechanosynthesis and after annealing. For sample designation, see Tab. I.

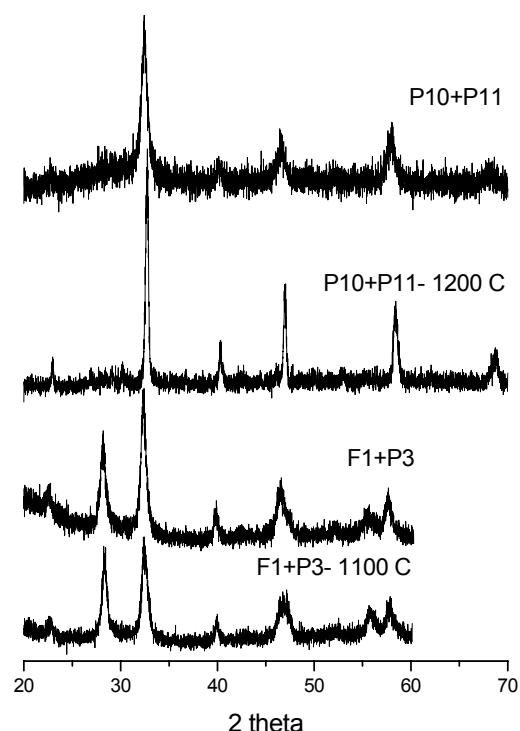


Fig. 2 Diffraction patterns of nanocomposites before and after sintering.

Sintering of both the individual complex compounds derived by mechanosynthesis and composites on their basis occurs in not quite usual manner: after heating is stopped, dilation of ceramics with a decrease of the density is observed. Optimal conditions (temperature and time) exist for the sintering of dense ceramics; they coincide with the conditions for obtaining ceramics with maximal conductivity, Fig. 4. A SEM image of sintered ceramics made from nanocomposite powder is shown in Fig. 5. The grain size is about ~ 400 nm, which approximately corresponds to the crystallite size estimated on the basis of broadening of reflections and to the mean size of aggregates which have not had enough time to grow noticeably during the short time of sintering. The volume of visible pores is small and corresponds to the measured density $\sim 96\%$.

The unusual sintering behavior of the powders of complex perovskites and fluorites derived by mechanosynthesis, exhibited by an extreme dependence of density and conductivity on the temperature, may be attributed to local chemical reactions – accelerated growth of some domains which inevitably are present in powders because of the complex composition and chemical non-uniformity [14-16], due to the formation of vacancies in other domains. According to the mechanism of sintering described in [16], rearrangement (enrollment, reorientation) of crystal particles as a whole, provided by surface diffusion contributes mainly to shrinkage, especially during elevation of T. When the heating rate $dT/dt = 0$, rearrangement of particles ceases; the growth of domains and grains via the volume diffusion mechanism, which gives almost no shrinkage even in usual binary oxides, becomes prevailing.

Table II Parameters of composites after sintering.

T _s , °C	Compo- sition		Density		Open porosity, %	Cell parameters, Å		Phase composition, %			Grain size, nm	
	1	2	g/cm ³	%		1	2	1	2	X	1	2
1100	F1	P3	6.112	-	0.1	5.518(4)	3.883(2)	41	40	19	98	171
1100	F1*	P3*	6,066	-	0.3	5.522(4)	3.886(1)	37	40	23	80	140
1100	F2	P2	4.436	66.1	22.5	a=4.0045(5); c=9.430(1)	3.888(1)	50	50	0	355	192
1100	F2	P4	6.203	-	0.1	-	-	0	0	100	-	-
1100	F2	P5	6.50	-	7.2	-	3.899(1)	0	60	40	-	90
1100	F2	P6	4.70		33.3	-	3.880(1)	0	60	40		102
1100	F2	P7	6.464	92.1	1.1	5.572(1)	3.877(1)	40	60	0	180	254
1100	F3	P4	6.091	-	3.4	-	-	0	0	100	-	-
1200	F4	P4	6.206	95.8	0.2	5.427(3)	3.850(1)	40	58	2	310	820
1200	P1	P4	5.138	80,8	11.9	3.8716(11)		97	3		196	
1200	P1	P6	6.575	95.9	0.13	a=5.500(2), c=13.347(3)		95	5		370	
1200	P8	P9	5.953	94.7	0.1	3.883(2)	3.875(1)	49	49	2	300	300
1200	P10	P11	5.817	91.6	1.58	3.876(2)	3.864(2)	49	49	2	400	400
1200	3F5	P6	6.970	97.0	0	5.419(2)	3.877(2)	78	21	1	230	130

*- Before mixing, powders were annealed at T= 400 °C. X – other phases

The scheme of relaxation during sintering, that is, rotation of a selected particle over angle Ψ in the potential field E of the surrounding particles in an ensemble is shown in Fig. 6. Under the action of the excess energy related to the surface of "solid-gas" and "solid-solid" types, (the last strongly depends on mutual orientation of crystallites), the particles choose different movement routes depending on conditions. For isothermal sintering, the formation of diffusion contacts between grains and their growth due to volume diffusion cause increasing of the potential barriers for particle rearrangement. As a result, a particle turns out to be in the nearest potential hole far from minimum, from which it cannot get out at the given temperature (the route is shown with a dashed line in Fig. 6). During this process, large pores are conserved in the bulk of the ceramics. Such pores do not disappear during further sintering but undergo coalescence together with grain growth (only subsurface pores have the possibility to go out in the surface). During fast heating of the system, when the particle size does not have enough time to change and oriented (topotaxial) contacts are not formed yet,

the possibilities of fluctuation overcoming of small potential barriers are maximal.

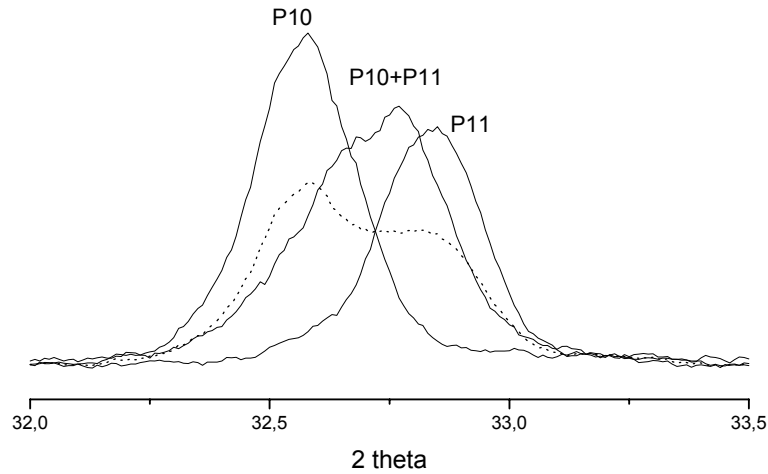


Fig. 3 Reflection (110) for initial perovskites and composite after sintering. The shape of the peak for the physical mixture is shown by a dashed line.

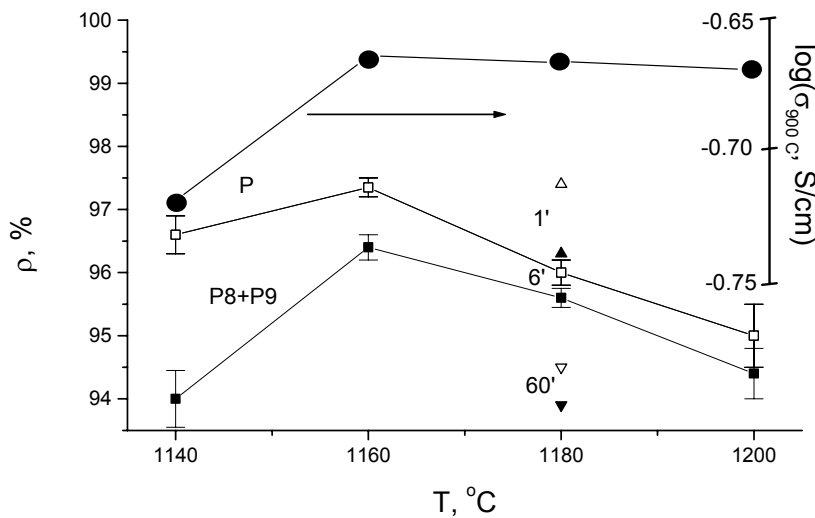


Fig. 4 Dependence of density and total conductivity of composite samples in air on the sintering temperature and time of exposure at the maximal temperature. P- single-phase perovskite with the chemical composition of the composite, derived by mechano-synthesis.

As a result, the particle has enough time to fall into a deep potential hole before the potential relief changes radically (the route is shown by a dotted line in Fig. 6). This complicated process of spatial and orientation rearrangement of the irregular shaped particles simultaneously with the formation of diffusion contacts and grain growth is evidently a cooperative one. Description of these complicated processes by equations in an analytical

form can hardly be possible. The methods of molecular dynamics are suitable for this purpose; they have developed during the recent years due to progress in computer techniques.

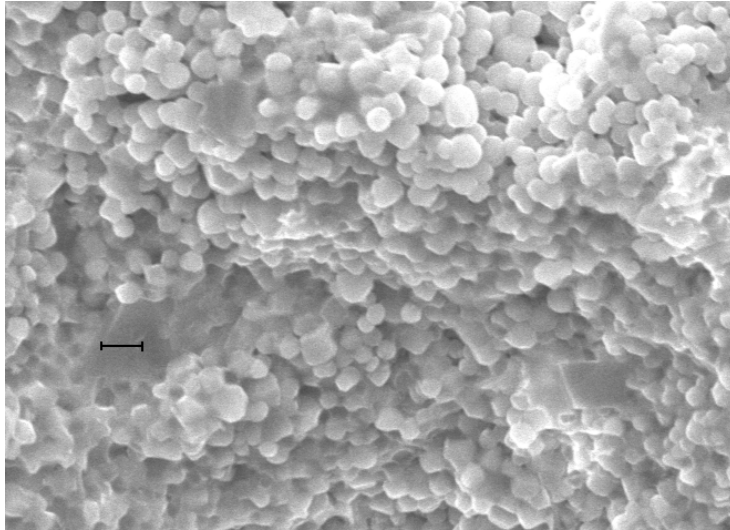


Fig. 5 Surface of P8+P9 composite after sintering at 1200 °C (mark: 1 μm).

The existing notions [21] concerning shrinkage during sintering, caused by simple volume diffusion leading to the approachment of the centres of contacting particles, have been developed for coarse powders and for model systems composed of two simple shaped bodies.

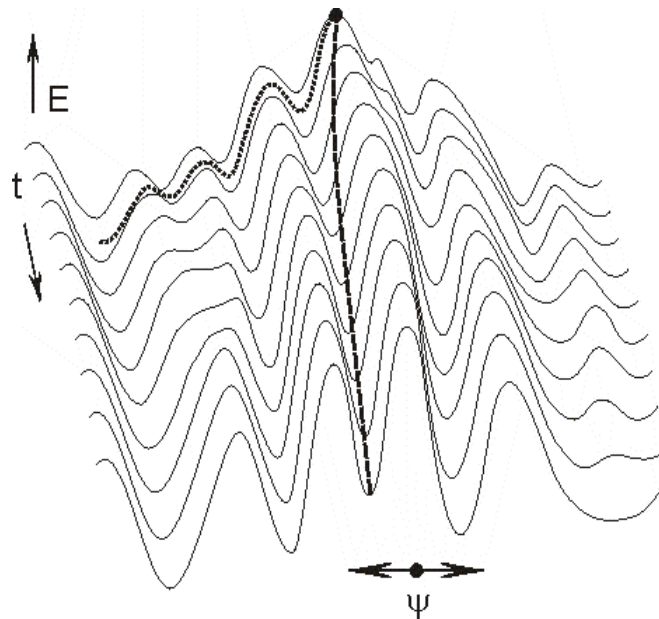


Fig. 6 A scheme of a potential relief of a selected crystal particle in ensemble and the change of the relief in isothermal conditions during sintering (For explanations, see text).

The effect of the particle rearrangement process on shrinkage for nano-sized powders should evidently increase strongly. Moreover, bulk diffusion and interdiffusion in nano-sized powder of a complex perovskite provides not shrinkage but dilation, Fig. 4. It should be noted that a strong deviation (up to 5-fold) between the experimentally measured rate of reorientation of large particles on single crystal substrate and the expected rate on the basis of diffusion mass transfer with the participation of dislocations in the contact zone was marked previously in [21].

Conclusion

Metastable complex oxides with fluorite and perovskite structures were derived by mechanosynthesis. Complex compounds with selected compositions keep their structure during sintering up to dense ceramics due to kinetic stabilization. A chemical interaction was observed during sintering of complex oxides composites in all systems but at different degrees. By optimizing the conditions of mixing individual phases and their sintering, it is possible to obtain ceramic composites with mixed conductivity for use in catalytic membrane reactors. Unusual behaviour of complex perovskites and fluorites during sintering was discovered: the existence of an optimal temperature and sintering time. A qualitative explanation of processes during sintering is proposed and the key role is attributed to rearrangement of crystal particles as a whole.

Acknowledgements

This work was supported in part by INTAS, Project No. 01-2162, and RFBR, 02-03-33330. The authors thank N. Uvarov for measurements of conductivity and A. Salanov for SEM investigations.

References

1. Y. Teraoka, H.M. Zhang, S. Furukawa, N. Yamazoe. *Chem. Lett.*, (1985) 1743-46.
2. Y. Teraoka, T. Nobunaga, K. Okamoto, N. Miura, N. Yamazoe. *Solid State Ionics*, 48 (1991) 207-12.
3. W.J. Weber, J.W. Stevenson, T.R. Armstrong, L.R. Pederson, J.J. Kingsley. *Mat. Res. Soc. Symp. Proc.*, 369 (1995) 395-400.
4. H. Takamura, M. Kawai, K. Okumura, A. Kamagawa, M. Okada. *Mat. Res. Soc. Symp. Proc.*, 756 (2003) EE.8.11.1-6.
5. C. Li, T. Hu, H. Zhang, Y. Chen, J. Jin, N. Yang. *J. Membr. Sci.*, 226 (2003) 1-7.
6. C. Navas, H.L. Tuller, H.-C. Loye. *Mat. Res. Soc. Symp. Proc.*, 548 (1999) 533-538.
7. B. Ma, U. Balachandran, C.-C. Chao, J.-H. Park. *Mat. Res. Soc. Symp. Proc.*, 453 (1997) 579-585.
8. P. Shuk, H.-D. Wiemhofer, et al. *Solid State Ionics*, 89 (1996) 179-196.
9. V.V. Kharton, A.V. Kovalevsky, A.P. Viskup, et al. *J. Electrochem. Soc.*, 147 (7) (2000) 2814-2821.
10. U. Nigge, H.-D. Wiemhofer, E.W.J. Romer. et al, *Solid State Ionics*, 146 (2002) 1630174.
11. Y. Shen, A. Joshi, M. Liu, K. Krist. *Solid State Ionics*, 72 (1994) 209.
12. J.K. Meen, O.A. Goksen, I.-C. Lin, K. Mukker, B. Nguyen. *Mat. Res. Soc. Symp. Proc.*, 658 (2001) GG9.14.1-6.
13. O.A. Goksen, J.K. Meen, A.J. Jacobson, D. Elthon. *Mat. Res. Soc. Symp. Proc.*, 658 (2001) GG4.7.1-5.
14. V.V. Zyryanov, N.F. Uvarov, V.G. Kostrovskii, V.A. Sadykov, T.G. Kuznetsova, V.A. Rogov, V.I. Zaikovskii, Y.V. Frolova, G.M. Alikina, G.S. Litvak, E.B. Burgina, E.M. Moroz, S. Neophytides. *Mat. Res. Soc. Symp. Proc.* 755 (2003) DD.6.27.1.
15. V. Zyryanov, N. Uvarov, V. Sadykov, G. M. Alikina, L. Ivashkevich, M. Ivanovskaya, S. Neophytides. *Proc. X APAM Topical Seminar "Nanoscience and technology"*, Novosibirsk, Russia, 2003, 173.

16. V. Zyryanov, N. Uvarov, V. Sadykov, Y. Frolova, M. Ivanovskaya, J.M. Criado, S. Neophytides. Proc. Of 6th Intern. Conf. on Catalysis in Membrane Reactors ICCMR-6, Lahnstein, Germany, July 6-9, (2004) 41-44.
17. V.V. Zyryanov. Chemistry for sustainable development, in press.
18. V.V. Zyryanov, in: (ed. by E.G. Avvakumov) "Mechanochemical synthesis in inorganic chemistry ". Novosibirsk: Nauka. 1991.
19. V.V. Zyryanov, V.G. Kostrovsky, A.A. Ivanova. Proceedings of the XVIII Mendeleev Congress on General and Applied Chemistry, Kazan, September 21-26, 1 (2003) 449.
20. V.V. Zyryanov, V.F. Sysoev, B.B. Bokhonov. USSR Inventor's Certificate No. 1477467, 1989.
21. Ya. E. Geguzin. Physics of sintering, Nauka, Moscow, 1984.

Резюме: Методом механосинтеза получены метастабильные твердые растворы комплексных оксидов с флюоритными и перовскитными структурами. Спеканием нанопорошков получена плотная керамика на основе метастабильных фаз. В процессе спекания композитов "перовскит + флюорит" и "перовскит + перовскит" установлены различные ступени химической реакции (взаимной диффузии). Показана возможность оптимизации состава, условий смешивания отдельных фаз и их спекание, приготовление керамических композитов для применения в мембранных каталитических реакторах. Установлено необыкновенное поведение комплексных перовскитов и флюоритов и определены оптимальная температура и время проведения спекания, для которых было дано и качественное толкование. Также было установлено, что перегруппировка тонких кристаллических частиц, как целого, играет главную роль при усадке.

Ключевые слова: Механосинтез, комплексные оксиды, перовскиты, флюориты, композиты, спекание, взаимная диффузия.

Садржај: Метастабилни чврсти раствори комплексних оксида са флуоритним и перовскитним структурама добијени су механосинтезом. Синтеровањем нанопрахова добијена је густа керамика на бази ових метастабилних фаза. Утврђени су различити ступени хемијске реакције (међудифузије) током синтеровања композита "перовскит+флуорит" и "перовскит+перовскит". Показано је да је могућа оптимизација састава, услова мешања појединачних фаза и њихово синтеровање, припрема керамичких композита за примену у каталитичким мембранским реакторима. Откривено је необично понашање комплексних перовскита и флуорита и одређени су оптимална температура и време синтеровања, за које је дато и квалитативно објашњење. Установљено је да реаранжирање финих кристалних честица као целине игра главну улогу у скупљању.

Кључне речи: Механосинтеза, комплексни оксиди, перовскити, флуорити, композити, керамика, синтеровање, међусобна дифузија.
